Korean J. Chem. Eng., 39(10), 2600-2614 (2022)
DOI: 10.1007/s11814-022-1192-2

pISSN: 0256-1115
eISSN: 1975-7220

Industrial symbiosis: Boron waste valorization through CO_2 utilization

Mehmet Çopur*, Turgay Pekdemir,†, Mehmet Muhtar Kocakerim***, Haluk Korucu***, and Rövşen Guliyev******

*Bursa Technical University, Chemical Engineering Department, 16310-Bursa, Turkiye
**Bolu Abant Izzet Baysal University, Chemical Engineering Department, 14030-Bolu, Turkiye
***Çankırı Karatekin University, Chemical Engineering Department, 18100-Çankırı, Turkiye
****Ardahan University, Environmental Engineering Department, 75000-Ardahan, Turkiye
(*Received 4 March 2022 • Revised 18 May 2022 • Accepted 30 May 2022*)

Abstract−Various wastes being generated globally and dumped on land by mineral processing activities pose great ecological and health problems. An example is the boron mineral beneficiation solid wastes. Even greater threat is anthropogenic carbon dioxide (CO_2) emissions among key causes of prevalent climate change. By this work, we propose a symbiotic solution to alleviate both environmental threats through recovering valuable boron products from boron wastes (BW), while also utilizing and sequestering CO_2 stably and permanently. This article presents the results on the effect of important operation parameters for the performance of such a process within the following ranges determined by preliminary tests: temperature: 20-60 °C, solid-to-liquid ratio: 0.1-0.5 g/ml, reaction time: 15-120 min, stirring speed: 300-700 rpm and particle size: 150-600 μm. CO_2 gas (99.9%) flow rate was maintained continuously at 1.57 l/min under atmospheric pressure. The important findings are (1) per ton of BW production of commercially valuable either (a) 310 kg sodium penta-borate or (b) 350 kg sodium penta-borate mixed with Na_2CO_3, depending on the process configuration, (c) 725 kg relatively pure $CaCO_3$, a potential source for precipitated calcium carbonate (PCC) and (d) 72 kg CO_2 utilization, (2) effective parameters for CO_2 utilization, in decreasing order are temperature, solid-to-liquid ratio and time, while stirring speed and particle size are ineffective within the range investigated and (3) the optimum operating conditions as: temperature: 60 °C, solid-to liquid ratio: 0.1 g/ml, time: 90 min, stirring speed: 500 rpm and particle size: <180 μm.

Keywords: Industrial Symbiosis, Boron Processing Wastes, Waste Valorization, Carbon Dioxide Sequestration, Carbon Dioxide Utilization

INTRODUCTION

The mineral processing industry, while commercially extracting valuable minerals and metals, generates globally large quantities of various seriously hazardous wastes. Among examples is concentrated (in terms of recoverable valuable content) solid waste produced by boron minerals beneficiation plants.

Boron minerals (i.e., tyncal, ulexite, colemanite, and kernite) are natural composites containing various proportions of boron oxide (B_2O_3), which determine the economic value and names for the boron products. According to Eti Mine [1,2], a Turkish mining corporate and the World Leader in boron reserves and production, boron minerals are found in 230 different forms in the nature. The total global (proven, probable and possible) reserve of boron minerals as of 2020 is around 4.5 billion tons (Bt), of which 3.3 Bt (approximately 73%) is in Turkey [3]. Major boron minerals together with their important characteristics are listed in Table 1 [4].

As it can be inferred from their chemical formula shown in Table 1, boron minerals are basic in character and, depending on the mineral type, can contain CaO, Na_2O and MgO [2]. Boron minerals are extracted from a mine mixed with clay and small amounts of carbonated minerals. The mine product is generally referred as "run-of-mine," which is subjected to beneficiation [5,6] for further downstream processing ensuring efficacious manufacturing. Available methods for boron minerals beneficiation have recently been reviewed by Powoe et al. [5]. Approximately 50-60% of run-of-mine solids is separated as waste [5,6].

Referred to as boron waste (BW), these run-of-mine solids are alkaline with high content of B_2O_3 (up to 31%), calcium (Ca), sodium (Na) and magnesium (Mg) [7-10]. BW, damped normally in the mine locations and currently without a commercial value, is usually small in particle size (<3 mm), which can potentially offer reduced cost for further crushing process that may be needed for

Table 1. Major boron minerals together with their important characteristics [4]

Boron minerals	Chemical formula	B_2O_3 Content (%)
Kernite	$Na_2B_{14}O_7 \cdot 4H_2O$	51.0
Colemanite[a]	$Ca_2B_6O_{11} \cdot 5H_2O$	50.8
Hydroboracite	$CaMgB_6O_{11} \cdot 6H_2O$	50.5
Pandermite	$Ca_4B_{10}O_9 \cdot 7H_2O$	49.8
Ulexite[a]	$NaCaB_5O_9 \cdot 8H_2O$	43.0
Tincal (Borax)[a]	$Na_2B_4O_7 \cdot 10H_2O$	36.5

[a]Dominant ones in Turkey in terms of reserve

†To whom correspondence should be addressed.
E-mail: turgay.pekdemir@ibu.edu.tr

later possible valorization and utilization. Alone in Bigadiç, Turkey, by the end of 2018, more than 4 million tons (Mt) of BW had already been stored in the field at the waste pools close to the plant with an annual generation rate of 250,000 tons (nearly 600,000 tons overall in Turkey). In China, another large boron producer, Zhang et al. [11] report a BW reserve of 35 Mt in 2016 with a growth rate of 1.6 Mt per year. As in Turkey, in China too, BW is generally stacked open-air near the ore plant. The storage and disposal of this BW contribute additional considerable costs to the operators due to needing allocation of large areas and further operations [11].

BW with a solubility of up to around 26 g/L in water at 25 °C [12], if left on the field open to the elements, can cause boron pollution in the soil and natural water sources, causing potentially serious environmental problems [7,13]. Due to concerns on human health, the World Health Organization (WHO) recommends a drinking water boron concentration lower than 2.4 mg/l [14]. Also, most crops are sensitive to boron presence and cannot tolerate if the concentration in irrigation water is higher than a certain level, depending on the boron sensitivity of crops [15]. Zaman et al. [16] report various values for boron concentration (ppm) for four classes of crops with regards to their boron tolerance: <0.5 satisfactory for all crops; 0.5-1.0 satisfactory for most crops; 1.0-2.0 satisfactory for semi-tolerant crops and 2.0-4.0 satisfactory for tolerant crops. According to the authors, fruit crops are especially boron sensitive. For example, even with concentrations of <0.5 ppm, for some stone fruit and citrus species, boron can reduce yields significantly. Therefore, BW accumulated around the mine area should be rendered harmless to avoid environmental contamination and resulting harm to crops and habitats of other life including humans.

Among options for avoiding environmental contamination, ways in which BW can be utilized beneficially as input to the manufacture of some value-added products have been emerging. Studies on the valorization and utilization of BW, however, have so far focused mainly on its use as additive in industries such as production of glass, porcelain, ceramic, terracotta, cement, brick, tiles including those for roofing and road construction, where BW is used either as substitute for primary raw clay building materials and/or to offset the demand for boric acid [11,13,17-28]. These studies to date have usually aimed to enhance the technological and structural properties of the final products, such as mechanical behavior, frost resistance, porosity, water absorption characteristics, durability and bulk density. These studies report that BW additives yield modified microstructure of the target materials, which enhances their technological performance positively. The readers who are interested in the degree of performance enhancement by BW additives and further details are referred to these studies referenced above.

To our knowledge to date, no studies so far have ever made efforts to recover commercially viable boron products, such as sodium penta-borate, while also symbiotically and simultaneously eliminating other environmentally harmful pollutants, such as carbon dioxide (CO_2).

It is now, also, widely perceived that CO_2 emission from anthropogenic sources is an effective greenhouse gas and the main contributor to the global warming, thus, to climate change [29]. In 2019 a special report on 1.5 °C by Intergovernmental Panel on Climate Change (IPCC) [30], in fact, had estimated that human activities, at the date of analysis, had already caused approximately 1.0 °C global warming since pre-industrial times. The report had warned that, if the emission increase was to continue at the same rate, global warming would most likely reach 1.5 °C between 2030 and 2052. The same report stated that there would still be several paths available for the world to utilize in curtailing that anticipated damage if acting immediately. The pathways, considering up to 50 scenarios and across four sectors, namely, energy, buildings, transport, and industry, included (a) CO_2 capture, utilization and storage (CDUS) in industry, (b) CCS in the power sector, (c) increasing the share of renewables in energy mix and electrification of and hydrogen use in transportation, (d) improving energy efficiency across all the sectors especially for buildings and (e) reducing emissions. The first two paths, if combined, can be referred to as carbon dioxide removal (CDR).

However, the most recent report by the IPCC [31] is far less optimistic and points out that the pathway to curtail global warming to 1.5 °C has now narrowed and presents only one plausible scenario to comply with that goal, which would require "unprecedented transformational change and rapid and immediate reduction of greenhouse-gas emissions." This means, in addition to the requirements to ensure large amounts of net-negative emissions and CDR, rapid elimination of fossil fuels from the relevant sectors while widescale adaptation of renewable energy and sharp reduction in the global energy demand.

Separately, the US Energy Information Administration (EIA) [32] predicts that, if it continues business as usual, by 2040 CO_2 releases can jump worldwide to over 43 billion metric tons. Indeed, the CO_2 concentration in the atmosphere has been progressively increasing in parallel to global industrial development. At the time of this writing, the global CO_2 trend in the air was reported as 419 ppm [33,34]. The COP26 in Glasgow recently ended with a draft agreement requesting nations, by the end of 2022, to revise their goals for cutting CO_2 emissions to limit global warming ideally to 1.5 °C by 2030 [35].

With this in mind, a wide range of studies have separately focused on the development of technological solutions for minimizing or alleviating consequential environmental problems through removing and safely locking harmful components away in environmentally benign forms. For example, capturing CO_2 from the point emission sources or directly from the air (DAC) and safely sequestering (storing) it underground and/or seabed to alleviate its global climate change impact.

There are several well-known sorts of methods, referred to as carbon capture and sequestration (Storage), shortly CCS, with varying maturity for this purpose, which may include absorption [36-40], adsorption [41-44] and membrane separation [45-48] operations either individually or their mixture in different combinations [49-60]. Sometimes these separation and purification methods are used as integrated with oxygen rich combustion (i.e., oxy-combustion) and gasification process [61-65]. CCS relevant topics have been widely researched, investigated, and reviewed. There are large numbers of specific and review-based literature in the field [66-73] as well as field applications varying in size from small pilots to full scale plants [74]. The separation and purification steps can produce almost pure CO_2 from the point source gas or the air. However, they

require significant amounts of processing plant investment (CAPEX) and energy cost (OPEX). This, for example, for power sector applications can consequently reduce the net electricity output of the power plant by as much as 30%, thus come at considerable financial and other resources burden [60].

Additionally, CCS chain requires laying out pipelines or use of shipping by sea or rail or road or mixture of these to transport the CO_2 to the places where all that CO_2 captured in pure form (99+%) regardless either from point emission sources or DAC should be stored either underground or seabed [75-80]. The storage places will require preparation work and post storage monitoring work to ensure safe storage [81-83]. Moreover, for various reasons, especially due to public acceptance, transporting large amounts of CO_2 and storing it underground or sea are perceived socially posing a serious risk and might even be a showstopper for CCS [84-86].

The estimated cost for the capture and storage/disposal from the emission sources such as power plants, even partially for a 85-90% CO_2, is prohibitively excessive and has been estimated to be as high as \$120/ton CO_2 depending on the source gas origin and CO_2 product purity [87,88]. Whereas for DAC, which can play important role in net zero pathways, the cost estimates are enormous being upwards of 600 \$/ton CO_2 [89-92].

On the other hand, environmental, legal, financial, and social considerations favor technological solutions and innovation to utilize CO_2 as a chemical raw material, for example, through processes dubbed as carbon dioxide utilization (CDU), in which CO_2 is used for beneficial purposes [93,94]. These kinds of processes, in comparison to simply capturing and storing CO_2 through CCS, have usually some advantages, such as better energy and material productivity and lower fossil fuel consumption and pollution generation or toxic chemical use [94,95]. CDU, in fact, has lately been considered among 100 radical innovation breakthroughs for the future in an independent expert report by the European Commission [96].

CO_2, being an acid gas, reacts with alkali and alkali-earth oxides and hydroxides [97]. This feature of CO_2 and this alkali material can be employed as an opportunity for CDU, for example, producing precipitated calcium carbonate (PCC) with large demand (an expected compound annual growth rate (CAGR) of 10.49% from 2020 to reach 6,443.60 Million \$ by 2026) from end-user industries such as paper, plastic, paint, adhesive & sealant, cosmetic, and electronics [98]. However, as PCC is mostly obtained by using lime, which is normally produced by calcinating limestone, thus, emitting CO_2 through the carbonation of a slurry of slaked lime ($Ca(OH)_2$), this process does not actually offer any net CO_2 utilization and thus advantage with respect to a net CO_2 sequestration. An alternative to this limestone method is a process proposed by a Japanese research group (Kakizawa method) [99], in which calcium is extracted from wollastonite mineral ($CaSiO_3$) using acetic acid. Others [100,101] expanded the Kakizawa method and showed that PCC production via this route could potentially yield a net CO_2 utilization of 0.34 kg/kg PCC, which translates to about 77% of maximum possible capacity of the material used.

Alternatively, reacting CO_2 with group I or II alkali metal minerals and/or wastes resulting from the production of carbonate products can also contribute to CO_2 sequestration and utilization. Recently, igneous rocks (e.g., serpentines and wollastonite) and industrial wastes (e.g., cement and lime kiln dusts, power plant fly ash and stainless steel slags) with large amounts of alkaline components, for example, magnesium oxide (MgO) and calcium oxide (CaO), have been used to bind CO_2 and safely store it in the form of carbonates through a process referred to as CO_2 mineralization [102-107]:

$$xMO{\cdot}ySiO_2{\cdot}zH_2O(s)+CO_2 \rightarrow xMCO_3(s)+ySiO_2(s)+zH_2O+Heat \quad (1)$$

where M stands for Ca and/or Mg.

In comparison to other CDU methods, CO_2 mineralization offers significant advantages in terms of sequestration capacity, permanency, safety and stability of the products [93]. In direct carbonization techniques, CO_2 in gaseous state is treated directly or in water with Ca or Mg-rich minerals or wastes [108]. Usually, the by-products are mainly $CaCO_3$ and Mg salts, which determines whether

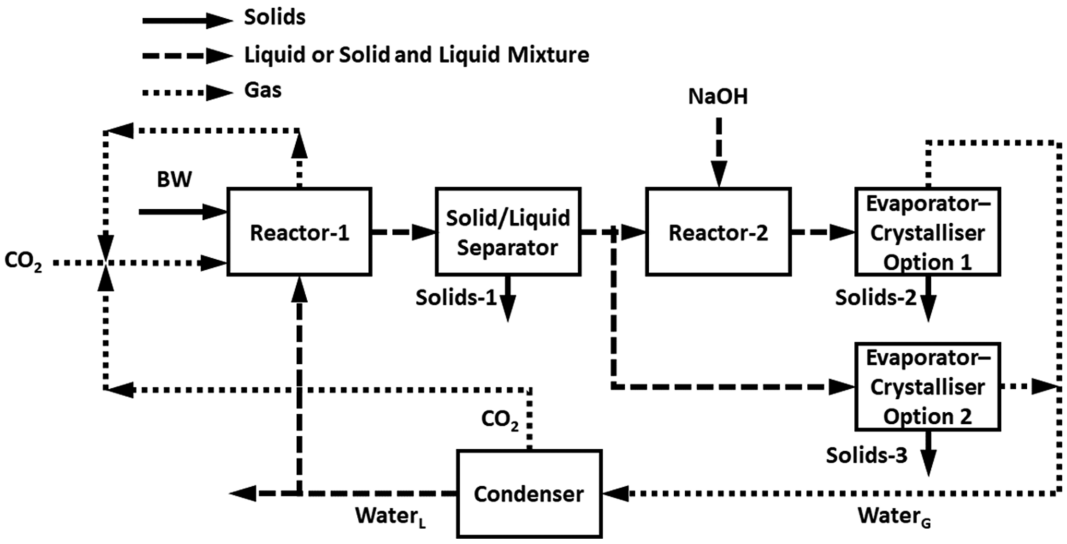

Fig. 1. Block diagram of the proposed process for boron waste (BW) valorisation through CO_2 utilisation.

the process can be economical.

Among the candidates of industrial wastes suitable for CO_2 mineralization, considering especially, as reported above, availability, is the BW with good level of alkalinity. Some of the authors of the current study, using concentrated ores, have already investigated the dissolution kinetics of boron minerals (i.e., ulexite, colemanite and tincal) in CO_2 or other acidic gas (e.g. SO_2) saturated waters with the sole purpose of maximizing the dissolution rate and recovering boron (i.e., B_2O_3) [109-111]. Building on this earlier experience, for the current study we aimed experimentally to investigate an industrial symbiotic solution, as depicted in Fig. 1, with the advantage of not only recovering valuable boron components from BW, but also creating additional value by utilizing CO_2 and locking it away stably and permanently. If BW is used for CO_2 mineralization in the way proposed by the present study, the benefits, in addition to eliminating mining related wastes causing environmental pollution, are given in Table 2.

The advantages of this proposed alternative symbiotic simultaneous BW valorization and CO_2 utilization route are obvious, considering relatively high monetary values of the products and waste elimination listed in Table 2. For example, sodium penta-borate with a value of about 1,500 $/ton (lower end price obtained from bulk suppliers as the reference [112]) can help significantly in enhancing not only the economics of the CO_2 utilization operation, but also elimination of environmental problems due to mining industrial waste. Additionally, the carbonated solid residue with some content of boron can be used as a cement replacement material with the advantage of increasing the long-term strength of the concrete [113-115]. With the EU carbon (CO_2) price in May 2021 hitting a record high 50 € per ton, the proposed CO_2 utilization process will also provide additional income through CO_2 emissions allowance scheme [116].

The estimated potential capacity of this route for CO_2 utilization, considering the global boron mineral reserves (4.5 Bt), can be up to about 0.62% of total CO_2 emissions in 2021 [117]. The authors, therefore, believe that the importance and novelty of the current study are its expected potential in (1) through symbiosis, creating products of value (up to 600 $/ton BW) from an industrial waste of great global warming threat, namely CO_2, and another waste in the form of BW with significant threat for water contamination, (2) reducing environmental problems (avoidance of CO_2 and boron pollution per ton of BW) and (3) yielding sustainable development through a circular economic activity.

EXPERIMENTAL DETAILS

The BW used in this investigation was obtained from the Bigadiç (Turkey) Boron Processing Works of Eti Mine company, which produces colemanite and ulexite minerals. The BW batch as received, which originated from ulexite enrichment operations, was first powdered and fractioned into particle-size ranges, as given in Table 3 together with their chemical analysis.

B_2O_3 content was determined by a common volumetric method [118], sodium (Na) and calcium (Ca) by a flame photometer (Sherwood 410), carbon (C) by a carbon analyzer (Eltra CS 500) and the others by XRF (Bruker S8 Tiger). The heating loss was determined by heating the samples to 900 °C in an oven (Carbolite-Gero RWF 11/23) and maintaining for 2 h at this temperature. The XRD (Rigaku Ultimate-IV) and Sem (ZEISS) of a selected BW sample (D_{100}: 600 μm) are given in Figs. 2 and 3, respectively. The

Table 2. Estimated benefits from the use of boron waste (BW) for CO_2 mineralisation by the method proposed by the present study

	Product	Mass kg/ton BW	Commercial value ($/ton)
Solids-1	Relatively pure $CaCO_3$ (including that originally available in BW), which can potentially be transformed to PCC (per Eqs. (9)-(11))	725	150
Solids-2	Commercially valuable boron compounds (e.g., sodium penta-borate mixed with Na_2CO_3, per Eqs. (13) and (14))	350	1,350
Solids-3	Commercially valuable boron compounds (e.g., sodium penta-borate, (per Eq. (11))	310	1,500
CO_2	Sequestrated/utilised CO_2 (per Eqs. (9)-(11))	72	56
Water	Treatable water source (per Eqs. (9)-(11))	75	0.5

Table 3. Chemical compositions of boron waste (BW)

Fractions D_{100} (μm)	Components (%)											
	B_2O_3	Na_2O	CaO	MgO	Fe_2O_3	Al_2O_3	As[a]	SO_4^{2-}	SiO_2	SrO	C	HL[b]
<600	23.06	1.84	25.91	6.78	0.09	0.20	75	0.11	9.37	1.15	7.51	31.21
<355	21.17	1.80	26.59	7.00	0.08	0.20	73	0.11	9.81	1.21	7.75	31.16
<250	20.31	1.81	26.97	6.92	0.09	0.22	70	0.12	9.93	1.19	7.90	31.30
<180	22.97	2.16	25.51	6.39	0.10	0.22	71	0.13	9.15	1.24	7.35	31.41
<150	23.20	2.12	24.59	6.80	0.09	0.21	70	0.14	9.73	1.07	7.35	31.38

[a]as ppm

[b]HL: Heating loss at 900 °C for 2 h

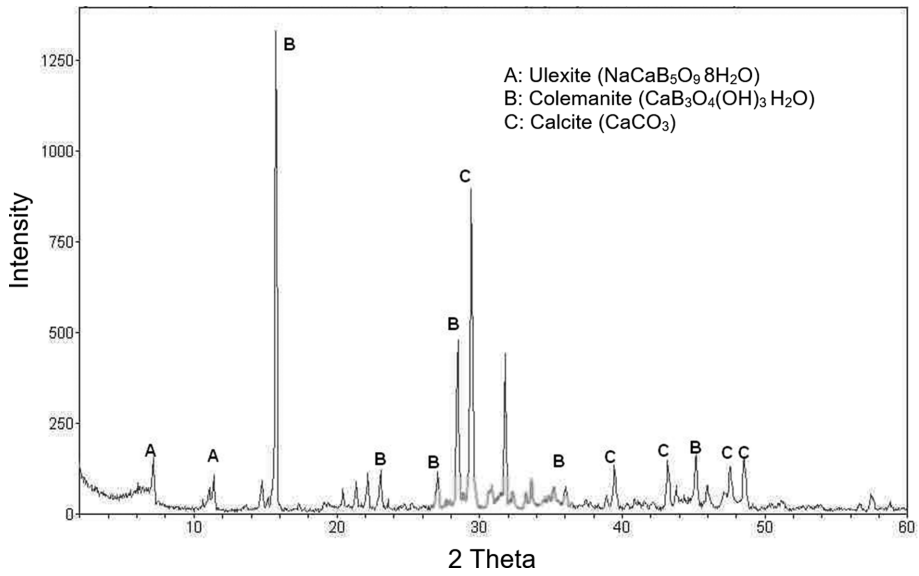

Fig. 2. XRD pattern of boron mineral waste (BW).

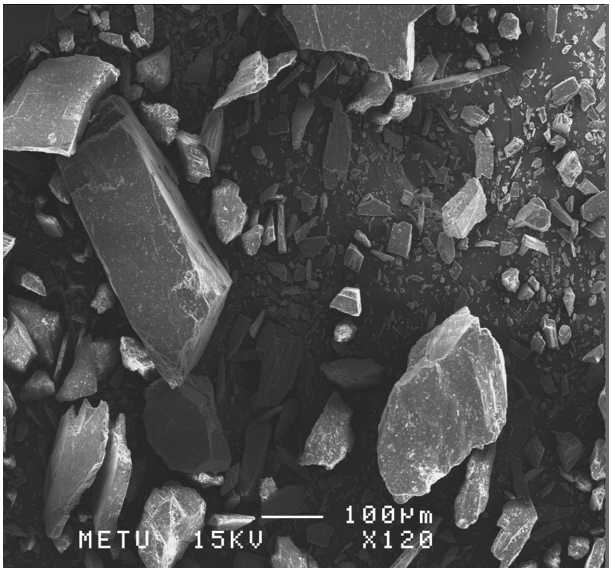

Fig. 3. SEM of <600 μm boron mineral waste (BW).

FTIR spectrum of some selected products was generated by a Thermo Fisher Nicolet IS50 spectrometer. Readers interested in the operation of, and material characterization by, these instruments are referred to [119-123]. From the XRD (Fig. 2) and chemical analysis (Table 3) of the samples, it is concluded that the BW contains ulexite, colemanite, calcite and some amount of clay minerals. As the chemical composition data given in Table 3, however, shows the presence of very little Na in comparison to that of Ca, it is inferred that ulexite content of BW is not that significant.

The CO_2 gas for the mineralization was of commercial quality with high purity (99.9%) and obtained from the Habas, Turkiye.

The parameters chosen for the mineralization tests were, as shown in Table 4 together with their level values, reaction temperature (A), particle size (B), stirring speed (C), solid-to-liquid ratio (D) and reaction time (E). The investigated ranges of the parameters depicted in Table 4 were determined through preliminary tests. The mineralization reaction was implemented in a jacketed spherical glass reactor of 500 mL total volume equipped with a stirrer, dip tube sparger system and refluxed graham condenser opened to the atmosphere. The wheel of the stirrer (impeller) was of PTFE with a semicircle shape of 18 mm radius and 3 mm thickness. The impeller was positioned into the reactor at 1 cm distance from the bottom surface by a shaft of 8 mm diameter connected to an electrical motor. The reaction temperature was controlled by a constant temperature circulator. The ambient pressure and temperature in the lab during the test period were around 610 mmHg and 21 °C, respectively.

Table 4. Parameters studied in the experiments and their levels and values

	Parameters	Levels and Values				
		1	2	3	4	5
A	Reaction temperature (°C)	20	30	40	50	60
B	Particle size (D_{100}: μm)	600	355	250	180	150
C	Stirring speed (rpm)	300	400	500	600	700
D	Solid-to-liquid ratio (g/ml)	0.1	0.2	0.3	0.4	0.5
E	Time (min)	15	30	60	90	120

For each experiment, a volume of 300 mL of distilled water was taken into the reactor (resulting in a 40% free space ratio) and saturated with a continuous flow of CO_2 gas stream. Following the saturation, determined by pH monitoring, CO_2 was fed continuously through the reactor at a constant flow of 1.7 l/min while the reactor was being heated. This rate of CO_2 stream was decided as the double the amount of that quantity of CO_2 required stoichiometrically to maintain the reactor content at saturation when operated with the highest solid-to-liquid ratio (0.5 g/ml) and shortest reaction time (15 min). This ensured that the reactor content was always CO_2 saturated regardless of the operating conditions. After

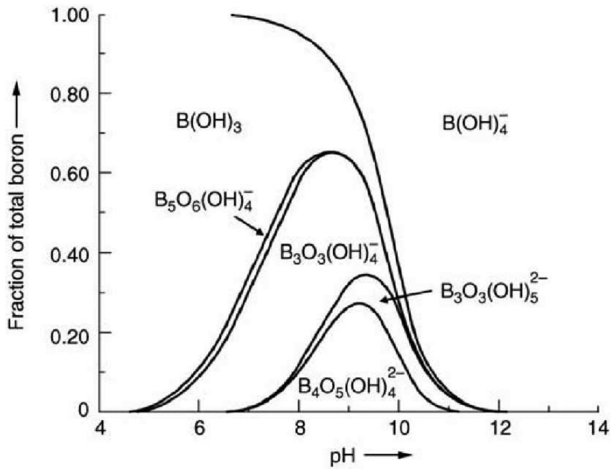

Fig. 4. The stoichiometric ratios of different borate species according to pH values [138].

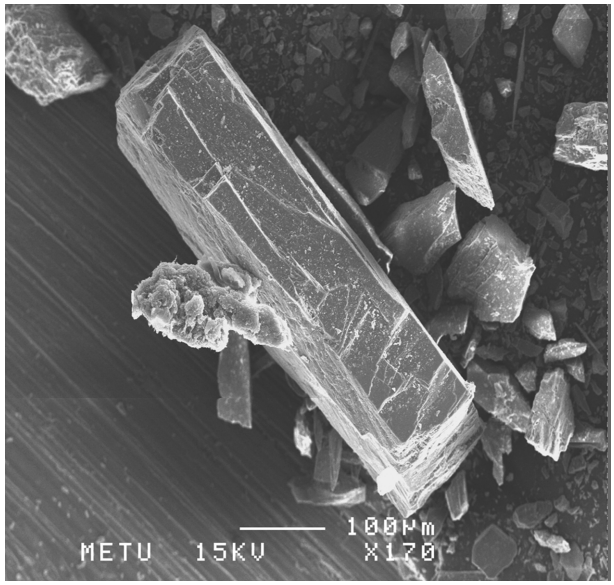

Fig. 6. SEM of solid residue (Solid -1) obtained with <600 μm boron mineral waste (BW).

the reactor content reached the target temperature, a predetermined BW sample, in accordance with the solid-to-liquid ratio shown in Table 4, was taken into the reactor and mixed with a predetermined mixing speed until the reaction time was completed. The pH observed throughout the current study for each test from shortly after the addition of the solids to the reactor until the end was between 6.5 and 7. Within this pH range, as shown in Fig. 4, the borate species in aqueous solution should be a mixture of $B_5O_6(OH)_4^-$, $B_4O_5(OH)_4^-$, $B_3O_3(OH)_4^-$ and H_3BO_3 [124-126]. Subsequently, the mixture in the reactor was filtered to separate remaining solids (residue: Solids-1 in Fig. 1) from the aqueous solution.

The chemical analyses of the residues for all the tests were implemented in the same manner as those for the feed BW samples. The XRD and SEM of a selected residue are given in Figs. 5 and 6, respectively.

The aliquot aqueous phase was heated in an evaporator-crystallizer (Option 2 in Fig. 1) followed by the precipitation and separation of solids (Solids-3 in Fig. 1). The XRD, FTIR and chemical analyses of this solid product obtained under optimum conditions are given in Fig. 7, Fig. 8 and Table 7, respectively.

An error analysis was implemented to estimate the accuracy of the results and error contributions from the uncertainties in the equipment and instrumentation used for the measurement of the independent variables affecting the CO_2 utilization performance results. It was found that the results could be in error up to 10% (equivalent to about 5% uncertainty). The repeatability with parallel tests and reproducibility with the tests carried out on different days were also investigated and found to be within 5% and 7%, respectively, of the mean values.

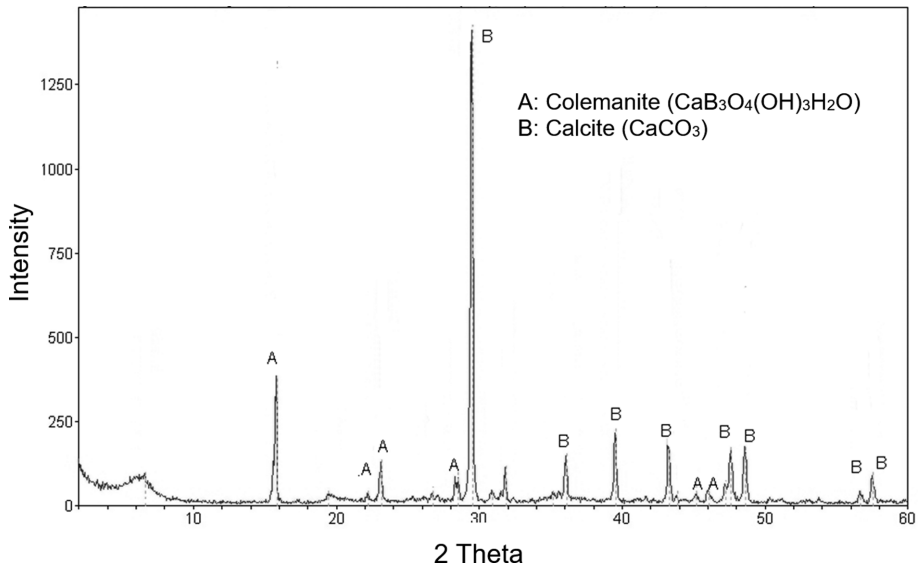

Fig. 5. XRD pattern of solid residue (Solid -1) obtained under optimum conditions.

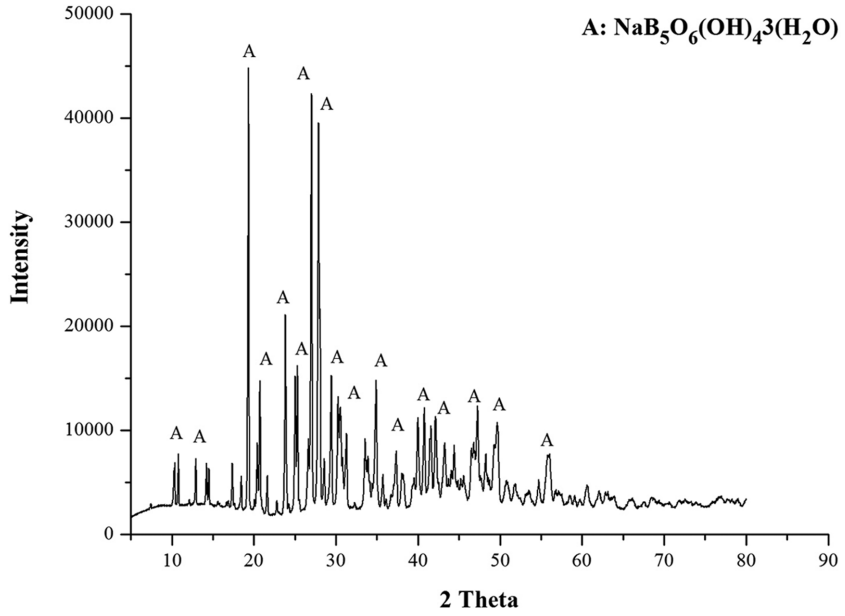

Fig. 7. XRD pattern of the solid product (Solid-3) obtained under optimum conditions.

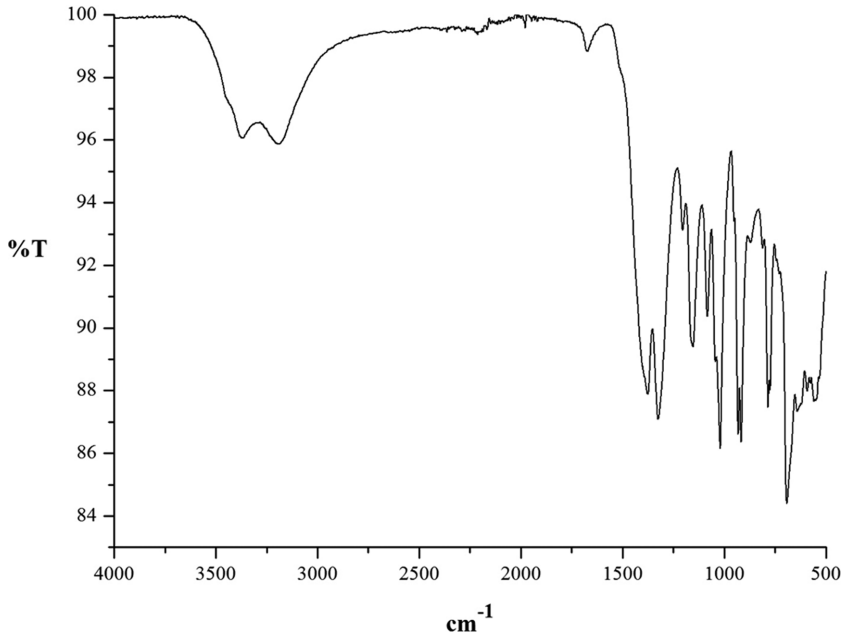

Fig. 8. FTIR spectrum of the solid product (Solid-3) obtained under optimum conditions.

TEST DESIGN METHODOLOGY

The optimization evaluations followed the Taguchi method with an experimental design method of L_{25} (5^5) orthogonal array (OA) as it was the most appropriate for the tests under investigation; five parameters each with five level values [127]. Main advantages of the Taguchi method are that it minimizes not only the experimental cost but also the variability around the target when bringing the performance value to that of target; also, the optimum working conditions determined from the laboratory work can also be reproduced in a real production environment. As the point by this study is not the Taguchi method but to determine optimum working conditions for the utilization of CO_2 while eliminating the environmental pollution and health risks due to BW, we will be content with giving only brief information that will enable a good understanding of the results. Those readers who are interested in the method itself and its application in similar investigations are referred to relevant studies in the literature [128-135].

The resultant test plan is shown in Table 5. Each test was repeated twice at different times. The larger-the-better principle was preferred as the optimization criterion for both CO_2 sequestered and B_2O_3 solubilised by using following equation [129,132]:

Table 5. L_{25} (5^5) Orthogonal experimental plan table

Run No	A	B	C	D	E
1	4	1	1	1	1
2	4	2	2	2	2
3	4	3	3	3	3
4	4	4	4	4	4
5	4	5	5	5	5
6	5	1	2	3	4
7	5	2	3	4	5
8	5	3	4	5	1
9	5	4	5	1	2
10	5	5	1	2	3
11	1	1	3	5	2
12	1	2	4	1	3
13	1	3	5	2	4
14	1	4	1	3	5
15	1	5	2	4	1
16	2	1	4	2	5
17	2	2	5	3	1
18	2	3	1	4	2
19	2	4	2	5	3
20	3	5	3	1	4
21	3	1	5	4	3
22	3	2	1	5	4
23	3	3	2	1	5
24	3	4	3	2	1
25	3	5	4	3	2

$$SN = -10\log\left(\frac{1}{n}\Sigma_{i=1}^{n}\frac{1}{Y_i^2}\right) \quad (2)$$

where SN is the performance characteristic, n number of repetitions performed for an experimental combination (=2) and Y_i performance (separately for CO_2 sequestered or B_2O_3 solubilized) value of the ith experiment. The performance value that corresponds to the optimal working conditions was predicted by using the balanced characteristic of the OA, using the addition model [132,134]:

$$Y_i = \mu + X_i + e_i \quad (3)$$

where μ is the overall mean of the performance value, X_i fixed effect of the parameter level combination used in ith experiment, and e_i the random error in ith experiment. As the value from this equation is a point estimate (prediction), calculated by using experimental data to determine whether the additive model is appropriate or not, the confidence interval of the prediction error should be evaluated. The validity of this hypothesis was verified by confirmation experiments conducted under optimal conditions and a procedure which is explained in one of our earlier study employing the same methodology [133].

The test data were analyzed by using an analysis of variance (ANOVA) computer software package for evaluating the effect of each parameter on the optimization criteria [131]. The larger-the better performance characteristics in Eq. (2) were used for the mineralization of CO_2. The F-test was used to determine the significance of the process operation parameters. The results are given in Table 6.

Table 6. Results of the analysis of variance (ANOVA) for CO_2 sequestration

	Parameters	SS	df	MS	F
A	Reaction temperature (°C)	324.63	4	81.16	41.62
B	Particle size (mm)	18.06	4	4.52	2.32
C	Stirring speed (rpm)	10.97	4	2.74	1.41
D	Solid-to-liquid ratio ($g.cm^{-3}$)	130.17	4	32.54	16.69
E	Time (min)	59.10	4	14.77	7.58
	Error	7.80	4	1.95	

SS: sum squares; **df**: degrees of freedom; **MS**: mean squares; **F**: F-test values

RESULTS AND DISCUSSION

A block diagram of the proposed route of CO_2 utilization route is shown in Fig. 1. The reactions taking place in the Reactor-1 are as follows:

The dissolution reactions of CO_2 in water [136,137]:

$$CO_2(g)+H_2O(l)\rightleftharpoons CO_2(aq)+H_2O(l) \quad (4)$$

$$CO_2(aq)+H_2O(l)\rightleftharpoons H_2CO_3(aq) \quad (5)$$

$$H_2CO_3(aq)+H_2O(l)\rightleftharpoons H_3O^+(aq)+HCO_3^-(aq) \quad (6)$$

$$HCO_3^-(aq)+H_2O(l)\rightleftharpoons H_3O^+(aq)+CO_3^{2-}(aq) \quad (7)$$

$$CO_2(aq)+CO_3^{2-}(aq)+H_2O(l)\rightleftharpoons 2HCO_3^-(aq) \quad (8)$$

However, considering that the pH values observed throughout the study were between 6.5 and 7, at any given time including the end of the reaction time, CO_2 speciation in the liquid phase will be H_2CO_3/HCO_3^- in portions of around 35/65 [136].

The reactions of CO_2 with BW: The ratios of ionic borate species expected to be present in the solution as function of pH are shown in Fig. 4 [138]. Within the pH range observed throughout the current study (between 6.5 and 7), the borate species in aqueous solution has been reported to be as $B_5O_6(OH)_4$, $B_4O_5(OH)_4^-$, $B_3O_3(OH)_4^-$ and $B(OH)_3$ (=H_3BO_3) [124-126]. Therefore, we anticipate that the reactions of CO_2 with BW (i.e., ulexite and colemanite in BW) in an aqueous media should proceed as follows with the borate products being mainly sodium penta- and three-borate:

$$2Na_2O\cdot 2CaO\cdot 5B_2O_3\cdot 16H_2O(s)+6H_2CO_3(aq) \rightleftharpoons 4CaCO_3(s)+2NaHCO_3(aq)+NaB_5O_6(OH)_4(aq) +NaB_3O_3(OH)_4(aq)+12H_3BO_3(aq)+15H_2O(l) \quad (9)$$

$$2CaO\cdot 3B_2O_3\cdot 5H_2O(s)+2H_2CO_3(aq)+2H_2O(l) \rightleftharpoons CaCO_3(s)+6H_3BO_3(aq) \quad (10)$$

If the remaining solids within the BW and the solid products from the reaction 10 above (Solids-1: mainly $CaCO_3$) are separated from the reactor effluent in a solid/liquid separator and then the aliquot aqueous phase is heated in an evaporator-crystallizer (Option 2), $NaHCO_3$ will break down and release some of already utilized CO_2 with Na being converted to sodium penta-borate:

Table 7. Chemical composition the solid product (Solid-3) obtained under optimum conditions

Components	B_2O_3	Ca	Na
%	57.43	0.046	6.38

$$2NaHCO_3(aq)+NaB_5O_6(OH)_4(aq)+NaB_3O_3(OH)_4(aq)+12H_3BO_3(aq)+15H_2O(l)\rightleftharpoons 4NaB_5O_6(OH)_43H_2O(aq)+2CO_2(g)+33H_2O(l) \quad (11)$$

The XRD and SEM of a selected residue (Solids-1) are shown in Figs. 5 and 6, respectively. It is apparent from these figures that the residue is mainly calcite ($CaCO_3$) and the ulexite in the BW is completely dissolved. The B_2O_3 analyses of the aliquot solution sample before being heated not only confirmed this, but also showed that 45% of colemanite was also dissolved. Also, evidenced by these figures, is that the dissolution of ulexite and colemanite has led to formation of rhombohedral calcite in agreement with the literature reporting that the similar conditions in a parent solution favor calcite formation and inhibits aragonite formation [139,140]. A large calcite crystal in Fig. 6 implies that new calcite formed deposit on the calcite crystals already existed in BW.

Further heating and evaporation of the aliquot aqueous phase will lead to a sodium penta-borate saturated solution, followed by precipitation and separation of sodium penta-borate crystals (Solids-3). The results of XRD, FTIR and chemical analysis of this solid product obtained under optimum conditions are given in Fig. 7, Fig. 8 and Table 7, respectively. These results, consistent with the literature [141-143], confirm the validity of reaction 11 and the product being sodium penta-borate ($NaB_5O_6(OH)_4{\cdot}3H_2O$), which may also be referred as Sborgite.

Whereas, if NaOH is added in a reactor (Reactor-2) to the liquid phase from the solid/liquid separator followed by a heating step in an evaporator-crystalliser (Option 1), $NaHCO_3$ will be converted to Na_2CO_3 as follows:

$$2NaHCO_3(aq)+NaB_5O_6(OH)_4(aq)+NaB_3O_3(OH)_4(aq)+12H_3BO_3(aq)+2NaOH(aq)\rightleftharpoons 4NaB_5O_6(OH)_43H_2O(aq)+2Na_2CO_3(aq)+18H_2O(l) \quad (12)$$

$$NaOH+5H_3BO_3\rightarrow NaB_5O_6(OH)_43H_2O(aq)+3H_2O(l) \quad (13)$$

Further heating and evaporation in this case will lead to a sodium penta-borate and sodium carbonate saturated solution, followed by precipitation and separation of a mixture of sodium penta-borate and sodium carbonate crystals (Solids-2). The Option 1 route offers the benefit of preventing the release of some portion of already captured CO_2 from the process back to the gas phase against the disadvantage of generated sodium penta-borate being mixed with sodium carbonate by a fraction of 0.11. Despite not being as pure as Solids-3, Solids-2 is still a good raw material with high demand potential for a number of manufacturing industries, such as production of special glass [144].

The vapor from the evaporator-crystallizer with small content of CO_2, for both Option-1 and Option-2 paths, can be condensed in a condenser. The non-condensables (mainly water saturated CO_2 of different quantity depending on whether Option-1 or Option-2 route is followed) can be fed back to the Reactor-1 as further passes. If reactions 9 to 13 above are studied carefully, it will become clear that the proposed process is a net water generator of approximately 75 kg water per ton of BW utilized. The excess water beyond that required by the process, being of relatively good quality, can be used for other on-site purposes.

As shown by the reactions in equations above, CO_2 in the solution is in the form of sodium bicarbonate ($NaHCO_3$). Accordingly,

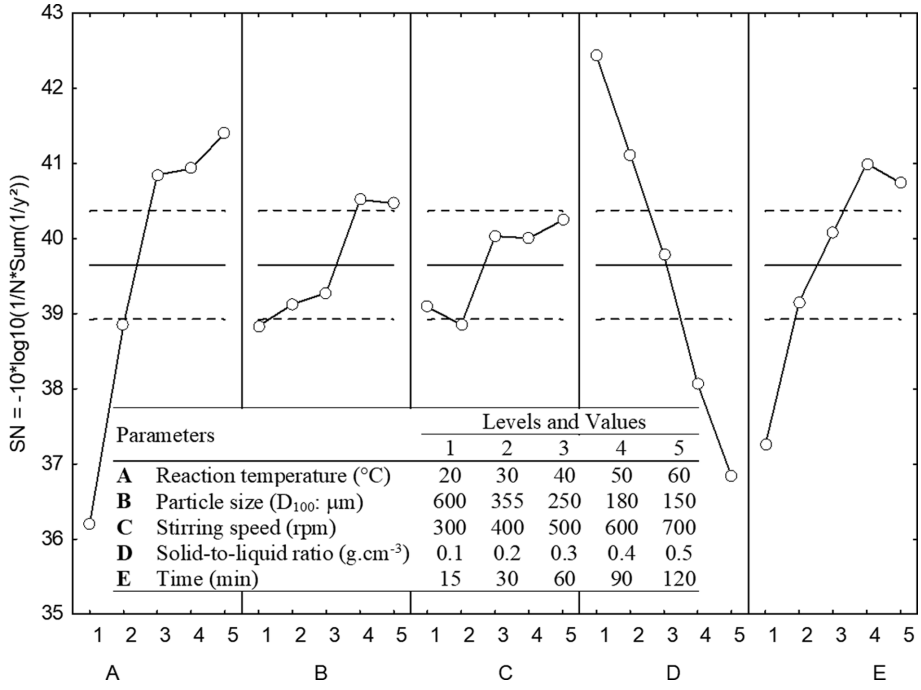

Fig. 9. The effect of each parameter on the optimization criteria for the solubilisation of B_2O_3.

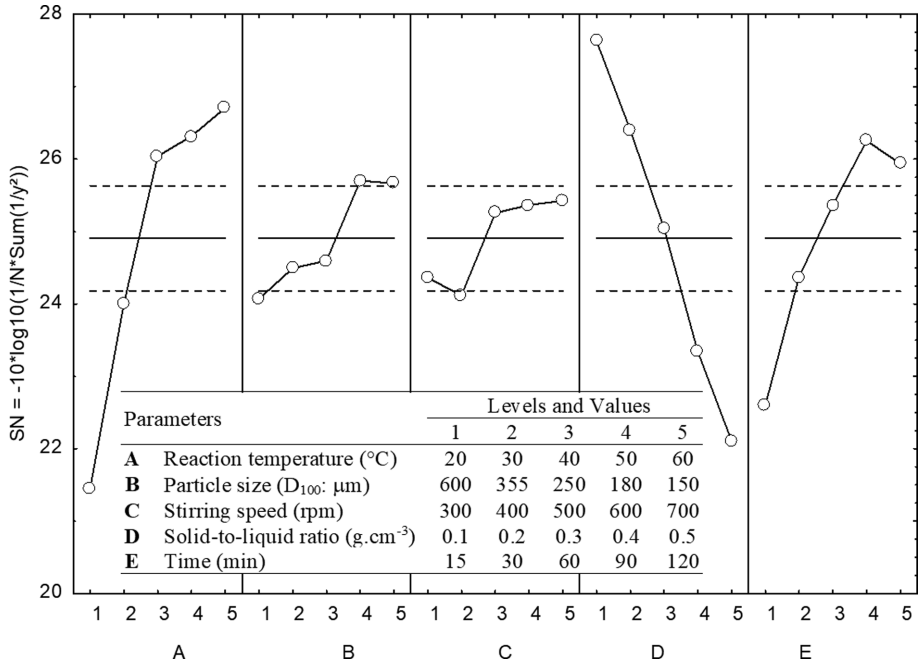

Fig. 10. The effect of each parameter on the optimization criteria for CO_2 utilisation.

the amount of CO_2 in the soluble form is proportional to the amount of sodium ion in the solution. The total captured CO_2 is, thus, the sum of CO_2 in the solid residue in the form of $CaCO_3$ ($M_{C(s)}$–$M_{C(org)}$) and as $NaHCO_3$ in the solution, which was calculated from the moles of Na^+ in solution using stoichiometry (as $(\frac{1}{2}M_{Na^+(aq)})$ from reactions 9 to 13). The total captured CO_2 mass (g) was then calculated as follows:

$$G_{CO_2}=\left[\frac{1}{2}M_{Na^+(aq)}+(M_{C(s)}-M_{C(org)})\right]44 \quad (14)$$

where $M_{Na^+(aq)}$ is the mole number of Na^+ ion in solution, $M_{C(s)}$ mole number of C in the solid residue and $M_{C(org)}$ mole number of C in the BW sample fed into the mineralization reaction.

The results from Eq. (14) were analyzed according to the optimization criteria (Eq. (2)) and are shown in Figs. 9 and 10 in the form of performance characteristics (SN). The optimal level for a given process parameter, in accordance with the methodology employed [133], is normally its value yielding highest SN value. In the working range, the parameter levels maximizing the performance value, according to Figs. 9 and 10, are a temperature of 60 °C (A_5), a particle size of <180 μm (B_4), a stirring speed of 700 rpm (C_3), a solid-to-liquid ratio of 0.1 g/ml (D_1) and a reaction time of 90 min (E_4). However, with regards to the stirring speed, considering the insignificant change in the SN value from 500 rpm to 700 rpm, but higher associated energy demand for the 700 rpm case, the optimum condition can be taken as 500 rpm.

Analysis of variance (ANOVA) was performed to determine the degree of effectiveness of CO_2 utilization parameters and their confidence levels, of which results are presented in Table 6. The confidence intervals are shown by the discontinuous lines in Figs. 9 and 10. As it can be seen from the statistical values in Table 6 (the higher the values higher the degree of the effectiveness of the parameter) and Figs. 9 and 10 (the steeper the curves and the degree by which they extend beyond the confidence interval lines higher the degree of the effectiveness of the parameter), in decreasing order, the reaction temperature, solid - liquid ratio and time, have significant impact on the CO_2 utilization, while particle size and the stirring speed, within the range investigated here, have insignificant effect.

The mechanism controlling the rate, in case of heterogeneous reactions, can be determined by considering the parameters that influence the reaction rate. For a process in which the stirring speed is more influential, the process rate is diffusion (mass transfer, that is, physically) controlled, whereas for the processes in which the temperature is more influential, the process rate is chemical reaction controlled. Therefore, it can be said that CO_2 utilization for the process under investigation is chemical reaction controlled. Physically controlled processes are more sensitive to particle size than chemically controlled processes, again due to being diffusion sensitive. Thus, the ineffectiveness of the particle size observed also supports that the CO_2 utilization process under investigation is reaction controlled.

The implication of these findings is that the process performance can be further improved if the reactor is operated at temperatures higher than 60 °C and solid-to-liquid ratios smaller than 0.1. The results discussed above imply that, for better CO_2 utilization rates, efforts can also be made to enhance the reactions, such as by means of catalysis. However, as the fact that the reaction between carbonate ions and calcium ions is very fast [145] and that the stirring speed affect is insignificant (Figs. 9 and 10), the carbonation (mineralization) reaction should thus dominantly be controlled by CO_2 solution equilibrium. The precipitation of calcite ($CaCO_3$) should, therefore, not favor higher temperatures since the

increased reaction temperature will reduce the solubility of CO_2 gas. In contrast, the solubility of ulexite and colemanite in BW in water should increase with temperature [146] and, thus, the availability of calcium ions in the solution for mineralization reaction. As result of these opposing effects of the temperature on the mineralization performance, it may be expected that the effect of temperature should be levelled or even declined at a certain temperature level. It appears that this temperature has not been reached within the range investigated here. A more favorable higher temperature should be sought to yield a better solubility of ulexite and colemanite in the BW, and thus a better reaction rate. This together with a cost analysis will be the subject of our further future studies of this promising CO_2 mineralization route.

The CO_2 captured under the optimal experimental condition was estimated to be approximately 72 kg CO_2 per ton BW, which, considering the global boron mineral reserves of 4.5 Bt, offers an estimated potential capacity for CO_2 utilization of up to about 0.5% of total yearly CO_2 emissions in 2021 [147]. According to the chemical analysis results given in Table 3, the average CaO content in the residue is 26%. If all this CaO in the residue were to react with CO_2 to produce $CaCO_3$, the amount of CO_2 reacted with BW would be 196 kg per 1 ton of BW. Based on this analysis, it might be erroneously thought that the overall CO_2 capture capacity was utilized only to a 37%. However, it must be noted that large portion of CaO reported in Table 3 (about 50%) in BW is actually in the form of free $CaCO_3$ without any capacity for CO_2 utilization. According to our analysis based on the stoichiometry of the reactions shown above and measurements of the soluble and non-soluble portions of the BW under reaction conditions, we estimated that the maximum CO_2 capture capacity of BW would be 91 kg CO_2 per ton BW. Thus, under the present test conditions, the utilized CO_2 capture capacity of BW is about 80%. Based on this, the CO_2 capture capacity can be enhanced to a maximum 0.62% of total yearly CO_2 emissions in 2021 by changing process operation conditions from the optimum as discussed above, for example, increasing the reactor temperature and/or decreasing solid-to-liquid ratio.

Studies following the expanded Kakizawa method [99] have reported a net CO_2 utilization of up to 340 kg/ton PCC [100,101]. However, based on the performance of the proposed method in the present study, it is possible to obtain a net CO_2 utilization of up to 710 kg/ton PCC. Note that CO_2 content in PCC can be maximum 440 kg/ton PCC. The balance for the present utilization of 710 kg/ton PCC is due to additional CO_2 being permanently utilized in the form of Na_2CO_3 while producing sodium penta-borate. Therefore, the CO_2 utilization capacity per kg of PCC proposed by the present study can potentially be about 110% higher in comparison to those reported in the literature [100,101].

To check the accuracy and reliability of the estimated results, in accordance with the recommendation in [148], two additional confirmatory CO_2 mineralization tests were carried out at different dates under the optimal operation conditions reported above. The average experimental CO_2 utilization value was found to be about 71 kg CO_2/ton BW. As the CO_2 sequestration values from the confirmatory tests are within the estimated confidence intervals (i.e., 95%), it can be inferred that the experimental error is within ±5% and that the results are reproducible. This confirms good consistency between estimated and experimental values and that parametric interactive effects were truly insignificant. It can, therefore, be stated that the addition model is sufficient to describe the dependence of this CO_2 sequestration process on the different operating parameters [127].

In this process, in addition to capturing CO_2 with the quantities mentioned above (72 kg CO_2 per ton BW), other useful and profitable products are generated. As shown in Table 2, these are, per ton BW, 310 kg sodium penta-borate and 725 kg relatively pure $CaCO_3$ (including that originally available in BW), which can potentially be transformed to PCC. The former is potentially a good alternative feed to produce useful other products. For instance, glass, fire-resistant plastics and rubbers, char promoters, anti-arcing agents, wood composites preservatives, etc. The latter can be used as an environmentally friendly alternative to the raw materials obtained from quarrying with significant environmental problems into the giant cement sector with huge global demand. The advantages of this proposed alternative symbiotic simultaneous BW valorization and CO_2 utilization route are obvious considering that the boron products (penta- and tri-borate) to be obtained in this mineralization process (see the reactions 9 to 13). Considerably high monetary values of the products (e.g., sodium penta-borate in pure form is sold for 1,500 $/ton [112]) can help significantly in enhancing not only the economics of the CO_2 utilization operation, but also elimination of environmental problems due to mining industries waste. Additionally, $CaCO_3$ produced in the operation is also marketable with market prices of 150 $ per ton [149,150]. Additionally, a CO_2 credit of about 4 $/ton BW can be obtained, which can further enhance the process economics.

CONCLUSIONS

This paper proposes a symbiotic route for the valorization of boron mineral processing solid wastes (BW) by CO_2 in aqueous solutions and then production of high market value of boron compounds, namely, sodium penta-borate, creating additional value by utilizing CO_2 and locking it away stably and permanently. This article reports the results from our initial study on the effect of the key operational parameters (temperature, solid-to-liquid ratio, reaction time, stirring speed and particle size) on the process performance. The main conclusion from this study is that this novel concept process for symbiotic valorisation of BW and CO_2 utilization is possible with products of high market value of boron compounds, namely, sodium penta-borate and precipitated calcium carbonate (PCC). Further conclusions from the study are:

1. The carbonated solids within the BW and solid products from the BW reactions with the CO_2 in aqueous solutions will lead to the generation of about 725 kg relatively pure $CaCO_3$ (Solids-1) per ton of BW, which can be separated from the reactor effluent and offer a very good raw material to produce PCC with a market value of 150 $/ton.
2. The BW reactions with the CO_2 in aqueous solutions will lead to valuable borate products of mainly sodium penta- and three-borate. If NaOH is added to this solution followed by a heating step (Option 1), $NaHCO_3$ will be converted to

Na_2CO_3 and further heating and evaporation will lead to the formation and separation of a mixture of about 350 kg sodium penta-borate and sodium carbonate crystals (Solids-2) per ton of BW with a market value of 1,350 $/ton.

3. Whereas, if the aqueous solution is heated without addition of NaOH (Option 2), $NaHCO_3$ will break down and release some of already utilized CO_2 and sodium three-borate converted to sodium penta-borate. Further heating and evaporation of the mixture will lead to a sodium penta-borate saturated solution followed by precipitation and separation of about 310 kg sodium penta-borate crystals (Solids-3) per ton of BW with a market value of 1,500 $/ton.
4. Solids-2, despite not being as pure as Solids 3, is still a good raw material with high demand potential for various manufacturing industries, such as production of special glass.
5. The proposed process is a net water generator of approximately 75 kg water per ton of BW utilized. The excess water beyond that required by the process, being relatively of good quality, can be utilized for other on-site purposes.
6. In decreasing order, the reaction temperature, solid - liquid ratio and time, have a significant impact on the CO_2 utilization, while particle size and the stirring speed, within the range investigated here, have insignificant effect. Therefore, the CO_2 utilization process under investigation is chemical reaction controlled.
7. In the working range, the parameter levels maximizing the performance value are a temperature of 60 °C (A_5), particle size of <180 μm (B_4), stirring speed of 700 rpm (C_3), solid-to-liquid ratio of 0.1 g/ml (D_1) and reaction time of 90 min (E_4). However, with regards to the stirring speed considering the insignificant change in the performance value from 500 rpm to 700 rpm, but higher associated energy demand for the 700 rpm case, the optimum condition can be taken as 500 rpm.
8. The process performance can be further improved if the reactor is to be operated at temperatures higher than 60 °C and solid-to-liquid ratios smaller than 0.1. However, the effect of the temperature on the mineralization performance is expected to be levelled or even declined at a certain temperature level. This temperature has not been reached within the range investigated here. We recommend a further investigation of the process with a cost analysis to find a more favorable higher temperature for better solubility of ulexite and colemanite in the BW, and thus a better reaction rate.
9. The CO_2 captured under the optimal experimental condition is approximately 72 kg CO_2 per ton BW, which, considering the global boron mineral reserves of 4.5 Bt, offers an estimated potential capacity for CO_2 utilization of up to about 0.5% of total yearly CO_2 emissions in 2021. With potential CO_2 credit, a value of about 4 $/ton BW can be obtained, which can enhance the process economics further.
10. The maximum CO_2 capture capacity of BW is around 91 kg CO_2 per ton BW. Thus, under the present test conditions, the utilized CO_2 capture capacity of BW is about 80%. Based on this, the CO_2 capture capacity can be enhanced to a maximum 0.62% of total yearly CO_2 emissions in 2021.

ACKNOWLEDGEMENTS

We are grateful to TUBITAK (The Scientific and Technological Research Council of Turkiye) for its financial support (108Y170) and Atatürk University, Erzurum, Türkiye, allowing this grant to be transferred to Çankırı Karatekin University, Çankırı, Turkiye to enable the completion of the research work.

NOMENCLATURE

A : operation test parameter label denoting temperature [°C]
ANOVA : analysis of variance [-]
B : Operation test parameter label denoting particle size [μm]
BW : run-of-mine solid wastes from boron enrichment processing [-]
C : operation test parameter label denoting stirring speed [rpm]
CAGR : compound annual growth rate [-]
CCS : carbon capture and sequestration [-]
CDR : carbon dioxide removal [-]
CDU : carbon dioxide utilization [-]
CDUS : carbon dioxide capture, utilization and storage [-]
COP26 : 26th The UN Climate Change Conference of the Parties in Glasgow, the UK [-]
D : operation test parameter label denoting solid-to liquid ratio [g/ml]
DAC : direct (CO_2) air capture [-]
df : degrees of freedom [-]
E : operation test parameter label denoting time [min]
e : Random Korean in an experimental test [-]
EIA : energy information administration [-]
EU : European Union [-]
F : F-test values [-]
G : total captured (utilised) CO_2 mass [g]
HABAS : Habaş Industrial and Medical Gases Production Industries Inc., Turkiye
HL : heating loss [-]
IPCC : Intergovernmental Panel on Climate Change [-]
M : number of moles of an element under question
MS : mean squares [-]
n : number of test repetitions performed for an experimental combination [-]
OA : orthogonal array [-]
PCC : precipitated calcium carbonate [-]
SN : performance characteristic [-]
SS : sum squares [-]
WHO : World Health Organization [-]
X : fixed effect of the test parameters' level combination used in an experimental test [-]
Y : performance value of an experimental test under a set of values of the test parameters [-]
μ : overall mean of the performance value [-]

REFERENCES

1. https://www.statista.com/statistics/264982/world-boron-reserves-by-major-countries/ (accessed 13 May 2022).

2. http://www.etimine.com/boron-minerals/ (accessed 13 May 2022).
3. http://www.etimine.com/boron-in-the-world/ (accessed 13 May 2022).
4. C. Helvaci, in *Encyclopedia of geology*, 2nd ed., A. Elias, Scott, David Eds., Academic Press (2021).
5. S.-P. B. Powoe, V. Kromah, M. Jafari and S. Chehreh Chelgani, *Minerals*, **11**, 318 (2021).
6. M. Sajid, G. Bary, M. Asim, R. Ahmad, M. Irfan Ahamad, H. Alotaibi, A. Rehman, I. Khan and Y. Guoliang, *Alexandria Eng. J.*, **61**, 3069 (2022).
7. E. Karadagli and B. Cicek, *Int. J. Appl. Ceram. Technol.*, **17**, 563 (2020).
8. B. Cicek, E. Karadagli and F. Duman, *Ceram. Int.*, **44**, 14264 (2018).
9. B. Cicek, E. Karadagli and F. Duman, *Constr. Build. Mater.*, **179**, 232 (2018).
10. İ. Kula, C. Gutsche, Y. Erdoğan, A. Fittschen and U. E. A. Fittschen, *Turkish J. Chem.*, **44**, 1244 (2020).
11. Y. Zhang, Q. Guo, L. Li, P. Jiang, Y. Jiao and Y. Cheng, *Materials (Basel)*, **9**, 416 (2016).
12. https://agriculture.borax.com/USBorax/media/assets/infographics/borates-mineral-solubility.pdf (2021) (accessed 13 May 2022).
13. Z. N. Kurt Albayrak and E. Turan, *Arab. J. Geosci.*, **14**, 1002 (2021).
14. W. Health, *World Health*, 4th ed., World Health Organization, Geneva (2011).
15. Y. Xu and J.-Q. Q. Jiang, *Ind. Eng. Chem. Res.*, **47**, 16 (2008).
16. M. Zaman, S. A. Shahid and L. Heng, *Guideline for salinity assessment, mitigation and adaptation using nuclear and related techniques*, Springer International Publishing, Cham (2018).
17. T. Kavas, *Build. Environ.*, **41**, 1779 (2006).
18. A. Olgun, Y. Erdogan, Y. Ayhan and B. Zeybek, *Ceram. Int.*, **31**, 153 (2005).
19. http://www.geology.cz/rroum/stazeni/2004_BAT_REFERENCE_DOCUMENT.pdf (2004) (accessed 13 May 2022).
20. I. Kula, A. Olgun, V. Sevinc and Y. Erdogan, *Cem. Concr. Res.*, **32**, 227 (2002).
21. A. Christogerou, P. Lampropoulou and E. Panagiotopoulos, *Constr. Build. Mater.*, **280**, 122493 (2021).
22. S. U. Bayca, *Theor. Found. Chem. Eng.*, **53**, 395 (2019).
23. A. Christogerou, T. Kavas, Y. Pontikes, C. Rathossi and G. N. Angelopoulos, *Ceram. Int.*, **36**, 567 (2010).
24. M. Marangoni, I. Ponsot, B. Cicek and E. Bernardo, *Adv. Appl. Ceram.*, **115**, 427 (2016).
25. A. Tunali, E. Ozel and S. Turan, *J. Eur. Ceram. Soc.*, **35**, 1089 (2015).
26. B. Cicek, A. Tucci, E. Bernardo, J. Will and A. R. Boccaccini, *Ceram. Int.*, **40**, 6045 (2014).
27. B. Cicek, L. Esposito, A. Tucci, E. Bernardo, A. R. Boccaccini and P. A. Bingham, *Adv. Appl. Ceram.*, **111**, 415 (2012).
28. S. Kurama, A. Kara and H. Kurama, *J. Eur. Ceram. Soc.*, **26**, 755 (2006).
29. J. G. J. Olivier, K. M. Schure and J. A. H. W. Peters, *PBL Netherlands Environ. Assess. Agency* (2017).
30. V. Masson-Delmotte, P. Zhai, H. O. Pörtner, D. Roberts, J. Skea, P. R. Shukla, A. Pirani, W. Moufouma-Okia, C. Péan, R. Pidcock, S. Connors, J. B. R. Matthews, Y. Chen, X. Zhou, M. I. Gomis, E. Lonnoy, T. Maycock, M. Tignor and T. Waterfield, Eds., https://www.ipcc.ch/site/assets/uploads/sites/2/2019/06/SR15_Full_Report_High_Res.pdf (2019) (accessed 13 May 2022).
31. https://report.ipcc.ch/ar6wg3/pdf/IPCC_AR6_WGIII_FinalDraft_FullReport.pdf (2022) (accessed 13 May 2022).
32. V. Masson-Delmotte, P. Zhai, H. O. Pörtner, D. Roberts, J. Skea, P. R. Shukla, A. Pirani, W. Moufouma-Okia, C. Péan, R. Pidcock, S. Connors, J. B. R. Matthews, Y. Chen, X. Zhou, M. I. Gomis, E. Lonnoy, T. Maycock, M. Tignor and T. Waterfield, *Summary for Policymakers: Global Warming of 1.5 °C* (2018).
33. ESLR, https://gml.noaa.gov/ccgg/trends/ (2021) (accessed 13 May 2022).
34. https://www.co2.eart (accessed 22 April 2022).
35. A. Åberg, T. G. Benton, A. Froggatt, A. Giritharan, N. Jeffs, D. Quiggin and R. Townend, *Chatham House*, 6 (2021).
36. B. Zhao, Y. Su, W. Tao, L. Li and Y. Peng, *Int. J. Greenh. Gas Control*, **9**, 355 (2012).
37. C. You and J. Kim, *Korean J. Chem. Eng.*, **37**, 1649 (2020).
38. S. Kumar and M. K. Mondal, *Korean J. Chem. Eng.*, **37**, 231 (2020).
39. A. Samanta, A. Zhao, G. K. H. Shimizu, P. Sarkar and R. Gupta, *Ind. Eng. Chem. Res.*, **51**, 1438 (2012).
40. Z. Zhang, T. N. G. Borhani and M. H. El-Naas, in *Exergetic, energetic and environmental dimensions*, 1st ed., İ. Dincer, C. Ö. Colpan and Ö. Kızılkan Eds., Elsevier (2018).
41. A. E. Creamer and B. Gao, *Environ. Sci. Technol.*, **50**, 7276 (2016).
42. C. M. O. González, E. M. C. Morales, A. de M. N. Tellez, T. E. S. Quezada, O. V. Kharissova and M. A. Méndez-Rojas, in *Handbook of greener synthesis of nanomaterials and compounds*, 1st ed., B. Kharisov and O. Kharissova Eds., Elsevier (2021).
43. R. Aniruddha, I. Sreedhar and B. M. Reddy, *J. CO_2 Util.*, **42**, 101297 (2020).
44. Y.-R. Lee, J. Kim and W.-S. Ahn, *Korean J. Chem. Eng.*, **30**, 1667 (2013).
45. M. K. Mondal, H. K. Balsora and P. Varshney, *Energy*, **46**, 431 (2012).
46. M. Zunita, R. Hastuti, A. Alamsyah, K. Khoiruddin and I. G. Wenten, *Sep. Purif. Rev.*, **51**, 261 (2022).
47. E. S. Sanni, E. R. Sadiku and E. E. Okoro, *Int. J. Chem. Eng.*, **2021**, 1 (2021).
48. M. Kárászová, B. Zach, Z. Petrusová, V. Červenka, M. Bobák, M. Šyc and P. Izák, *Sep. Purif. Technol.*, **238**, 116448 (2020).
49. M. C. Duke, B. Ladewig, S. Smart, V. Rudolph and J. C. Diniz da Costa, *Front. Chem. Eng. China*, **4**, 184 (2010).
50. X. Wang and C. Song, *Front. Energy Res.*, **8**, 560849 (2020).
51. M. A. A. M. Abdah, M. Mokhtar, L. T. Khoon, K. Sopian, N. A. Dzulkurnain, A. Ahmad, Y. Sulaiman, F. Bella and M. S. Su'ait, *Energy Reports*, **7**, 8677 (2021).
52. M. Alidoost, A. Mangini, F. Caldera, A. Anceschi, J. Amici, D. Versaci, L. Fagiolari, F. Trotta, C. Francia, F. Bella and S. Bodoardo, *Chem. - A Eur. J.*, **28**, e202104201 (2022).
53. B. Freeman, P. Hao, R. Baker, J. Kniep, E. Chen, J. Ding, Y. Zhang and G. T. Rochelle, *Energy Procedia*, **63**, 605 (2014).
54. A. T. Nakhjiri and A. Heydarinasab, *J. Ind. Eng. Chem.*, **78**, 106 (2019).
55. C. A. Scholes, S. E. Kentish and A. Qader, *Sep. Purif. Technol.*, **237**, 116470 (2020).
56. M. Scholz, B. Frank, F. Stockmeier, S. Falß and M. Wessling, *Ind. Eng. Chem. Res.*, **52**, 16929 (2013).

57. P. Shao, Z. He, Y. Hu, Y. Shen, S. Zhang and Y. Yu, *Chem. Eng. J.*, **435**, 134957 (2022).
58. L. Lavagna, G. Syrrokostas, L. Fagiolari, J. Amici, C. Francia, S. Bodoardo, G. Leftheriotis and F. Bella, *J. Mater. Chem. A*, **9**, 19687 (2021).
59. M. Reina, A. Scalia, G. Auxilia, M. Fontana, F. Bella, S. Ferrero and A. Lamberti, *Adv. Sustain. Syst.*, **6**, 2100228 (2022).
60. W. Zhang, Y. Xu and Q. Wang, *Energy*, **241**, 122524 (2022).
61. D. Jansen, M. Gazzani, G. Manzolini, E. van Dijk and M. Carbo, *Int. J. Greenh. Gas Control*, **40**, 167 (2015).
62. O. Omoregbe, A. N. Mustapha, R. Steinberger-Wilckens, A. El-Kharouf and H. Onyeaka, *Energy Reports*, **6**, 1200 (2020).
63. A. I. Osman, J. K. Abu-Dahrieh, N. Cherkasov, J. Fernandez-Garcia, D. Walker, R. I. Walton, D. W. Rooney and E. Rebrov, *Mol. Catal.*, **455**, 38 (2018).
64. A. I. Osman, T. J. Deka, D. C. Baruah and D. W. Rooney, *Biomass Convers. Biorefinery*, 1 (2020).
65. P. Wienchol, A. Szlęk and M. Ditaranto, *Energy*, **198**, 117352 (2020).
66. T. Wilberforce, A. G. Olabi, E. T. Sayed, K. Elsaid and M. A. Abdelkareem, *Sci. Total Environ.*, **761**, 143203 (2021).
67. M. Bui, C. S. Adjiman, A. Bardow, E. J. Anthony, A. Boston, S. Brown, P. S. Fennell, S. Fuss, A. Galindo, L. A. Hackett, J. P. Hallett, H. J. Herzog, G. Jackson, J. Kemper, S. Krevor, G. C. Maitland, M. Matuszewski, I. S. Metcalfe, C. Petit, G. Puxty, J. Reimer, D. M. Reiner, E. S. Rubin, S. A. Scott, N. Shah, B. Smit, J. P. M. Trusler, P. Webley, J. Wilcox and N. Mac Dowell, *Energy Environ. Sci.*, **11**, 1062 (2018).
68. A. I. Osman, M. Hefny, M. I. A. Abdel Maksoud, A. M. Elgarahy and D. W. Rooney, *Environ. Chem. Lett.*, **19**, 797 (2021).
69. N. Shreyash, M. Sonker, S. Bajpai, S. K. Tiwary, M. A. Khan, S. Raj, T. Sharma and S. Biswas, *Energies*, **14**, 4978 (2021).
70. N. S. Sifat and Y. Haseli, *Energies*, **12**, 4143 (2019).
71. P. Gabrielli, M. Gazzani and M. Mazzotti, *Ind. Eng. Chem. Res.*, **59**, 7033 (2020).
72. I. Ghiat and T. Al-Ansari, *J. CO_2 Util.*, **45**, 101432 (2021).
73. C. Chao, Y. Deng, R. Dewil, J. Baeyens and X. Fan, *Renew. Sustain. Energy Rev.*, **138**, 110490 (2021).
74. J. Ma, L. Li, H. Wang, Y. Du, J. Ma, X. Zhang and Z. Wang, *Engineering*, In press (2022) DOI:10.1016/j.eng.2021.11.024.
75. E. Smith, J. Morris, H. Kheshgi, G. Teletzke, H. Herzog and S. Paltsev, *Int. J. Greenh. Gas Control*, **109**, 103367 (2021).
76. IEAGHG, *The Status and Challenges of CO2 Shipping Infrastructures. Technical Report 2020-10* (2020).
77. National Petroleum Council, *Meeting the Dual Challenge - A Roadmap to At-Scale Deployment of Carbon Capture, Use and Storage* (2020).
78. P. Psarras, J. He, H. Pilorgé, N. McQueen, A. Jensen-Fellows, K. Kian and J. Wilcox, *Environ. Sci. Technol.*, **54**, 6272 (2020).
79. T. K. Righetti, *Oil Gas, Nat. Resour. Energy J.*, **3**, 907 (2017).
80. D. L. Sanchez, N. Johnson, S. T. McCoy, P. A. Turner and K. J. Mach, *Proc. Natl. Acad. Sci.*, **115**, 4875 (2018).
81. [IEA] - International Energy Agency, *Special Report on Carbon Capture, Utilisation and Storage: CCUS in Clean Energy Transitions* (2020).
82. https://ec.europa.eu/energy/maps/pci_fiches/PciFiche_12.4.pdf (accessed 22 April 2022).
83. Energy Technologies Institute, https://www.eti.co.uk/programmes/carbon-capture-storage/strategic-uk-ccs-storage-appraisal (2016) (accessed 13 May 2022).
84. K. Arning, J. Offermann-van Heek, A. Sternberg, A. Bardow and M. Ziefle, *Environ. Innov. Soc. Transitions*, **35**, 292 (2020).
85. F. Mulyasari, A. K. Harahap, A. O. Rio, R. Sule and W. G. A. Kadir, *Int. J. Greenh. Gas Control*, **108**, 103312 (2021).
86. K. Arning, A. Linzenich, L. Engelmann and M. Ziefle, *Energy Clim. Chang.*, **2**, 100025 (2021).
87. Power Technology, https://www.power-technology.com/features/carbon-capture-cost/ (accessed 13 May 2022).
88. Adam Baylin-Stern and Niels Berghout, https://www.iea.org/commentaries/is-carbon-capture-too-expensive (accessed 13 May 2022) (2021).
89. https://www.iea.org/reports/direct-air-capture-3 (2022) (accessed 13 May 2022).
90. THE Verge, https://www.theverge.com/2022/4/7/23013822/carbon-dioxide-removal-direct-air-capture-climate-change (accessed 13 May 2022).
91. https://www.iea.org/reports/direct-air-capture-2022 (2022) (accessed 13 May 2022).
92. THE VERGE, https://www.theverge.com/2022/4/4/23009804/united-nations-climate-change-report-greenhouse-emissions-2030-ipcc (accessed 13 May 2022).
93. T. Pekdemir, *Carbon dioxide utilisation: Closing the carbon cycle: 1st ed.*, Elsevier Inc. (2014).
94. F. M. Baena-Moreno, M. Rodríguez-Galán, F. Vega, B. Alonso-Fariñas, L. F. Vilches Arenas and B. Navarrete, *Energy Sources, Part A Recover. Util. Environ. Eff.*, **41**, 1403 (2019).
95. A. Schreiber, P. Zapp and W. Kuckshinrichs, *Int. J. Life Cycle Assess.*, **14**, 547 (2009).
96. P. Warnke, K. Cuhls, U. Schomoch, L. Daniel, L. Andresscu, B. Dragomir, R. Gheirghiu, C. Baboschi, A. Curaj, M. Parkkinen and O. Kuusi, *100 Radical Innovation Breakthroughs for the future*, European Commission (2019).
97. G. Montes-Hernandez, M. Bah and F. Renard, *J. CO_2 Util.*, **35**, 272 (2020).
98. https://www.reportlinker.com/p06087127/Precipitated-Calcium-Carbonate-Market-Research-Report-by-Type-by-End-User-by-State-United-States-Forecast-to-Cumulative-Impact-of-COVID-19.html?utm_source=GNW (2021) (accessed 13 May 2022).
99. M. Kakizawa, A. Yamasaki and Y. Yanagisawa, *Energy*, **26**, 341 (2001).
100. S. Teir, S. Eloneva and R. Zevenhoven, *Energy Convers. Manag.*, **46**, 2954 (2005).
101. R. Zevenhoven, S. Eloneva and S. Teir, *Catal. Today*, **115**, 73 (2006).
102. A. H. A. Park and L. S. Fan, *Chem. Eng. Sci.*, **59**, 5241 (2004).
103. E. Nduagu, T. Björklöf, J. Fagerlund, J. Wärn, H. Geerlings and R. Zevenhoven, *Miner. Eng.*, **30**, 75 (2012).
104. A. L. Harrison, I. M. Power and G. M. Dipple, *Environ. Sci. Technol.*, **47**, 126 (2013).
105. L. C. Pasquier, G. Mercier, J. F. Blais, E. Cecchi and S. Kentish, *Environ. Sci. Technol.*, **48**, 5163 (2014).
106. N. Kemache, L. C. Pasquier, E. Cecchi, I. Mouedhen, J. F. Blais and G. Mercier, *Fuel Process. Technol.*, **166**, 209 (2017).
107. J. H. Lee and J. H. Lee, *Korean J. Chem. Eng.*, **38**, 1757 (2021).

108. E. R. Bobicki, Q. Liu, Z. Xu and H. Zeng, *Prog. Energy Combust. Sci.*, **38**, 302 (2012).
109. M. S. Bingöl and M. Çopur, *J. CO_2 Util.*, **29**, 29 (2019).
110. M. Ozekmekci and M. Copur, *J. CO_2 Util.*, **42**, 101321 (2020).
111. H. Elçiçek and M. M. Kocakerim, *Brazilian J. Chem. Eng.*, **35**, 111 (2018).
112. https://www.indiamart.com/proddetail/sodium-pentaborate-1211448991.html (accessed 13 May 2022).
113. I. Kula, A. Olgun, Y. Erdogan and V. Sevinc, *Cem. Concr. Res.*, **31**, 491 (2001).
114. A. Olgun, T. Kavas, Y. Erdogan and G. Once, *Build. Environ.*, **42**, 2384 (2007).
115. N. Uçar, A. Çalık, M. Emre and I. Akkurt, *Indoor Built Environ.*, **30**, 1827 (2021).
116. N. Buli, K. Abnett and S. Twidale, https://www.reuters.com/business/energy/eu-carbon-price-tops-50-euros-first-time-2021-05-04/ (2021) (accessed 13 May 2022).
117. IEA, https://www.iea.org/news/global-carbon-dioxide-emissions-are-set-for-their-second-biggest-increase-in-history (2021 (accessed 13 May 2022).
118. M. Hollander and W. Rieman, III, *Ind. Eng. Chem. Anal. Ed.*, **17**, 602 (1945).
119. S. Xu, Q. Gao, C. Zhou, J. Li, L. Shen and H. Lin, *Mater. Chem. Phys.*, **274**, 125182 (2021).
120. Z. Huang, Q. Zeng, Y. Liu, Y. Xu, R. Li, H. Hong, L. Shen and H. Lin, *J. Membr. Sci.*, **640**, 119854 (2021).
121. B. Chen, H. Xie, L. Shen, Y. Xu, M. Zhang, H. Yu, R. Li and H. Lin, *J. Membr. Sci.*, **640**, 119820 (2021).
122. L. Rao, X. You, B. Chen, L. Shen, Y. Xu, M. Zhang, H. Hong, R. Li and H. Lin, *Chemosphere*, **288**, 132490 (2022).
123. J. Fang, Y. Chen, C. Fang and L. Zhu, *Sep. Purif. Technol.*, **281**, 119876 (2022).
124. J. L. Anderson, E. M. Eyring and M. P. Whittaker, *J. Phys. Chem.*, **68**, 1128 (1964).
125. Y. Zhou, C. Fang, Y. Fang and F. Zhu, *Spectrochim. Acta - Part A Mol. Biomol. Spectrosc.*, **83**, 82 (2011).
126. N. Kabay, M. Bryjak and N. Hilal, *Boron separation processes*, Elsevier, New York (2015).
127. C. Y. Nian, W. H. Yang and Y. S. Tarng, *J. Mater. Process. Technol.*, **95**, 90 (1999).
128. M. S. Phadke, R. N. Kackar, D. V. Speeney and M. J. Grieco, *Bell Syst. Tech. J.*, **62**, 1273 (1983).
129. J. J. Pignatiello, *IIE Trans. (Institute Ind. Eng.)*, **20**, 247 (1988).
130. Phillip J Ross, *Taguchi techniques for quality engineering: loss function, orthogonal experiments, parameter and tolerance design*, 2nd Ed., McGraw-Hill, New York (1996).
131. G. Taguchi, *System of experimental design; quality resources*, Unipub-Kraus International Publications, New York (1987).
132. M. S. Phadke, *Quality engineering using robust design*, Prentice-Hall, Englewood Cliffs, New Jersey (1989).
133. M. Çopur, T. Pekdemir, C. Çelik and S. Çolak, *Ind. Eng. Chem. Res.*, **36**, 682 (1997).
134. M. N. Islam and A. Pramanik, *J. Adv. Manuf. Syst.*, **15**, 151 (2016).
135. G. S. Peace, *Taguchi methods, a hands-on approach to quality engineering*, Addison-Wesley, New York (1995).
136. W. G. Mook, in *Environmental isotopes in the hydrological cycle - principles and applications*, W. G. Mook Ed., International Atomic Energy Agency and United Nations Educational, Scientific and Cultural Organization (2001).
137. F. Barzagli, C. Giorgi, F. Mani and M. Peruzzini, *J. CO_2 Util.*, **22**, 346 (2017).
138. D. M. Schubert, in *Ullmann's encyclopedia of industrial chemistry*, Wiley-VCH Verlag GmbH & Co. KGaA (2015).
139. Y. Kitano, M. Okumura, M. Idogake and M. Idogaki, *Geochem. J.*, **13**, 223 (1979).
140. Y. Kitano, M. Okumura and M. Idogaki, *Geochem. J.*, **12**, 183 (1978).
141. http://www.webmineral.com/data/Sborgite.shtml#.YmsQUtpBw2z (2012) (accessed 13 May 2022).
142. N. V. Chukanov, *Infrared spectra of mineral species*, Springer Netherlands, Dordrecht (2014).
143. S. Merlino, *Acta Crystallogr. Sect. B Struct. Crystallogr. Cryst. Chem.*, **28**, 3559 (1972).
144. E. D. Spinosa, D. T. Hooie and R. B. Bennett, *Summary report on emissions from the glass manufacturing industry*, Environmental Protection Technology Series. EPA, Ohio (1979).
145. F. Pacheco-Torgal, C. Shi, A. P. Sanchez, A. Palomo Sánchez and F. P. Torgal, *Carbon dioxide sequestration in cementitious construction materials*, Woodhead Publishing (2018).
146. D. M. Schubert, in *Ullmann's encyclopedia of industrial chemistry*, Wiley-VCH Verlag GmbH & Co. KGaA, Weinheim, Germany (2015).
147. https://www.iea.org/news/global-carbon-dioxide-emissions-are-set-for-their-second-biggest-increase-in-history (2021) (accessed 13 May 2022).
148. R. Davis and P. John, in *Statistical approaches with emphasis on design of experiments applied to chemical processes*, InTech (2018).
149. https://www.made-in-china.com/products-search/hot-china-products/Calcium_Carbonate_Price.html (accessed 13 May 2022).
150. https://www.alibaba.com/showroom/pure-calcium-carbonate-price.html (accessed 13 May 2022).